Jurnal Tribologi 43 (2024) 86-103

Jurnal Tribologi
Website : jurnaltribologi.mytribos.org
e-issn: 2289-7232

Thermal stability of laser modified die insert surface in hot press forming of 22MnB5

Norhafzan Bariman [1,2], Syarifah Nur Aqida Syed Ahmad [1*], Izwan Ismail [3], Khairil Che Mat [2]

[1] Faculty of Mechanical and Automotive Engineering Technology, Universiti Malaysia Pahang Al-Sultan Abdullah, Pahang, MALAYSIA.
[2] Department of Mechanical Engineering, Politeknik Muadzam Shah, Pahang, MALAYSIA.
[3] Faculty of Manufacturing and Mechatronic Engineering Technology, Universiti Malaysia Pahang Al-Sultan Abdullah, Pahang, MALAYSIA.
*Corresponding author: aqida@umpsa.edu.my

KEYWORDS

Laser modified surface
Die insert
Hot press forming
Temperature history
Martensite

ABSTRACT

Laser surface modification enhanced steel hardness properties from refined grain structure. Despite its superior properties, the thermal stability of fine grain structure is questionable as its metastable phase. This study investigates laser-modified die insert surface in hot press forming (HPF) of 22MnB5 steel blanks. The modified die insert was characterised for surface integrity, metallographic study, and thermal stability. From the findings, the laser-modified die inserts surface exhibits a thickness range between 0.10 and 0.33 mm with a refined grain structure of 1.02 µm, and respective surface roughness and subsurface hardness of 1.89-3.89 µm and 684.4-793.7 $HV_{0.1}$. The blanks that formed using laser-modified die inserts exhibit a higher martensite structure of 74.8-80.6% with an average hardness of 508.1 $HV_{0.1}$, while the high-strength steel blanks formed using the as-received surface inserts consist of 58.7 % martensite structure with 386.6 $HV_{0.1}$ hardness. Correlating the thermal stability of laser modified surface, the refined grain structure in laser modified die inserts surface was retained during the HPF process though the die insert surface was exposed to heated blank at temperatures above 600 °C. These findings are significant to design HPF die inserts surface for a prolonged lifecycle.

Received 17 July 2024; received in revised form 9 September 2024; accepted 28 September 2024.
To cite this article: Bariman et al., (2024). Thermal stability of laser modified die insert surface in hot press forming of 22MnB5. Jurnal Tribologi 43, pp.86-103.

1.0 INTRODUCTION

Hot Press Forming (HPF) has become one of the most important technologies in the automotive manufacturing sector. It produced ultra-high-strength components of automobile structures up to 1500 MPa due to the quenching effect during forming. During hot working processes, the metal is shaped in a die under high pressure. The critical phase of the process is the quenching stage, where the die's cooling channels rapidly dissipate heat from the hot metal. This rapid cooling transforms the metal's microstructure from austenite to martensite, significantly enhancing its tensile strength. Prolonged contact between die surfaces and the working material at high pressure and temperature caused extensive material strain led to plastic deformation of the die (Emamverdian et al., 2021). Changes in the surface topography of tool steel material due to high temperature have caused large variations in friction and wear of HPF tool steel materials (Zheng et al., 2016). Cyclic heating and cooling cause cracks on the die surface, which require repairs to prolong its service. These surface changes necessitate frequent repairs to maintain die performance. To address these issues, the convenient and economical methods were modification or remanufacturing without buying a new die.

Laser surface modification is widely used as a remanufacturing process, especially for repairing cracks on moulds and die surfaces. It's a unique tool with a micron-size heat source for high-precision surface modification. It produces new properties on the surface of the substrate, which improves toughness, hardness and corrosion, thus reducing wear resistance and thermal stress due to homogenous and ultrafine structure from localised rapid heating and cooling (Norhafzan et al., 2016). When grain size is refined, other properties such as ultimate tensile strength, yield strength, and elongation are improved. Several studies conducted for micro-alloyed with Ti and C successfully refined the grain size by changing the grain shape from columnar to equiaxed (Liu et al., 2019). In the author's previous study, laser melted surface exhibits an excellent bonding between modified layer and substrate material, enhanced hardness, absence of flaws, produced new mechanical properties and thermally stable layer (at temperatures below 600 ℃) (Norhafzan et al., 2016).

Apart from high thermal conductivity, the HPF die surface requires high hardness properties at elevated temperatures. At a high cooling rate, blank materials can be transformed into martensitic structures with high strength, which are affected by parameters such as die cooling channel, quenching time, water flow rate and water temperature (Du et al., 2018). However, the strength reduced when the austenitisation temperature decreased below 775 ^{o}C (Mori et al., 2017). The rapid cooling rate requires a high thermal conductivity die surface that depends on its grain structure and chemical composition to transfer heat from austenitized blank material to the die surface. High thermal conductivity can prevent material from premature degradation due to substantial overheating caused heat from the material diffuse very fast (Burger et al., 2016). However, changes in surface topography of tool steel material due to high temperature have caused large variations in friction, and wear of HPF tool steel materials (Zheng et al., 2016).

Despite its superior properties, the thermal stability of refined grain structure from laser modification has been a concern, specifically above 650 ℃. Hardness properties of metastable surface like laser modified layer and nanostructures coatings decreased proportionally to the annealing period (Aqida et al., 2009), (Gordillo et al., 2017; Sun et al., 2017). Due to its metastable phase, the grains move and merge into larger grains at elevated temperatures. Nevertheless, applying high pressure as a strengthening method (Han & Yi, 2022), can be applied to retain the grain structure of laser modified surface at high working temperatures. Besides, refined grain structure in the modified steel surface affects lattice thermal conductivity. Lattice thermal

conductivity depends on crystallinity, grain structure, chemical composition and temperature (Peet et al., 2011). Varying the grain boundaries significantly changed phonon scattering (Nagarjuna et al., 2020), atom configurations and bonding, thus exhibit different thermal conductivity behaviour (Fujii et al., 2020).

In this research, tool steel surface is modified using laser melting process for enhanced hardness properties and thermal stability during hot press forming. Prototype HPF die inserts were designed with laser modified surfaces that responding to pressure and austenitized 22MnB5 steel blanks. Thermal distribution was recorded to determine cooling rates effect on microstructural changes in 22MnB5 steel blanks. These findings contribute to the analysis of HPF die insert surface integrity, chemical composition effect on thermal conductivity and properties of 22MnB5 steel after HPF processes. The combination of wear resistance, high strength and thermal stability can increase significantly the die lifetime.

2.0 EXPERIMENTAL PROCEDURE

The material investigated in this study was ASSAB 8407 supreme, an AISI H13 compatible tool steel with chemical composition given in Table 1. Laser modification was conducted on die inserts surface of 70×33×8 mm dimension using JK300HP Nd:YAG twin laser source with 1064 nm wavelength and pulse processing mode. Table 2 shows the laser parameters setting used to modify the die inserts, with argon gas flow at 30 kPa pressure to protect the sample surface from oxidation during laser melting. The laser processing setup is shown by a schematic diagram in Figure 1. The sample surface was prepared with methanol before laser processing to avoid contaminations and ensure its cleanliness. Argon gas at 30 kPa pressure was used to protect the sample surface from oxidation during laser melting. The Nikon Tool Maker Microscope (MM400/800) was used to observe the laser spot size. Five laser spots without any overlapping were measured before starting the laser melting process to determine the exact spot size. The result from microscope observation shows the average spot size was 0.7 mm. Then laser beam was focused to 0.7 mm spot size onto the sample surface with an average power of 100 W. The laser head was consistently in a vertical position of 90° and was moved linearly in the x-y direction during the melting process of the sample surface.

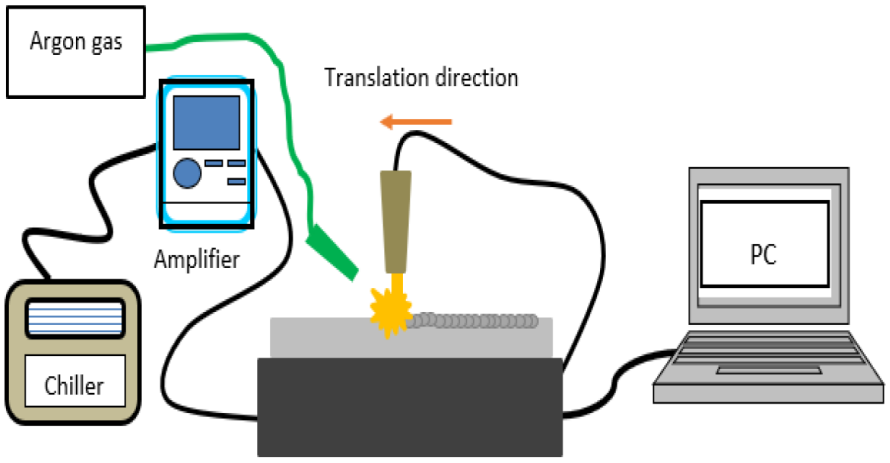

Figure 1: Schematic diagram of laser surface melting process setup.

Die fabrication was conducted using CNC machining for precision. The ASSAB 8407 steel block was cut using wire cut and using CNC milling into 140 x 70 x 38 mm for die insert holders upper and lower as shown in Figure 2(a) and (b), while Figure 2(c) shows die inserts after machining into 70×33×8 mm. The screw hole of laser modified die insert was drilled using die sinking process due to its high hardness properties

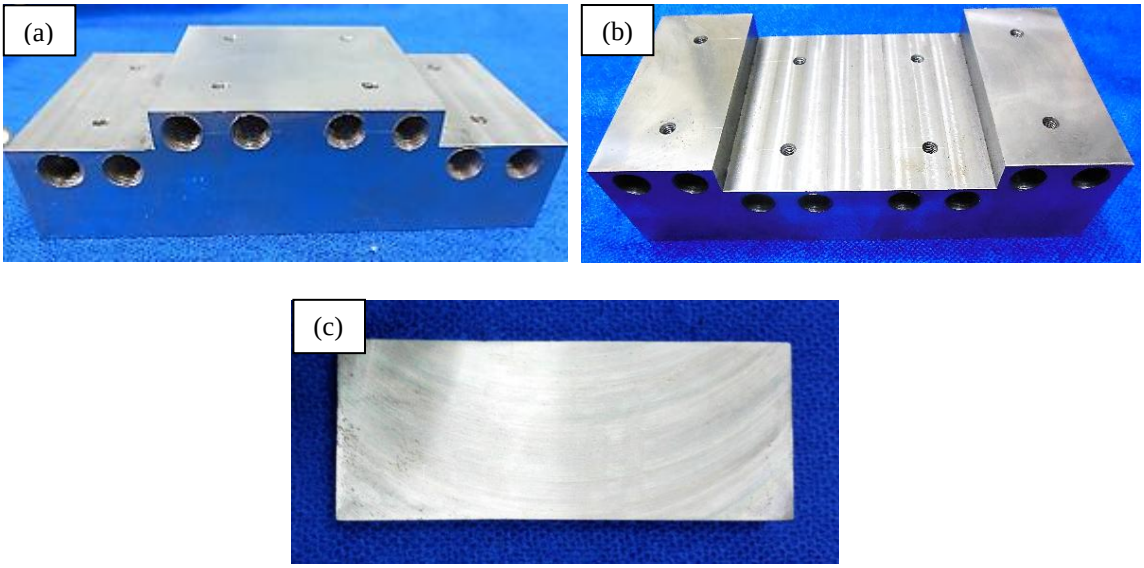

Figure 2: As-machined geometry of (a) upper and (b) lower die insert holder, and (c) die insert surface condition before laser melting.

The surface and subsurface of the laser-modified die insert surface were then characterised for surface morphology, roughness, modified layer depth, hardness properties, metallographic study, and chemical composition. The modified layer depth, metallographic study and chemical composition were conducted using Hitachi TM3030Plus scanning electron microscope integrated with energy-dispersive x-ray spectroscopy (EDXS). The microstructure composition in 22MnB5 blanks was analysed using ImageJ software with threshold analysis. Hardness properties were measured using Wilson hardness tester with Vickers diamond indenter and 100 kN load, while surface roughness was measured using 7061 MarSurf PS1 Roughness Tester.

Table 1: Chemical composition of ASSAB 8407/ AISI H13 steel.

Element (wt.%)									
C	**Si**	**S**	**Ti**	**V**	**Cr**	**Mn**	**Mo**	**Ni**	**Fe**
9.907	0.704	0.003	0.006	0.234	3.578	0.143	0.466	0.021	Bal.

Table 2: Parameter setting for laser surface modification of AISI H13 steel.

Parameter	**Input**
Average power	100 W
Peak power	1700 – 2500 W
Pulsed repetition frequency, PRF	50 – 70 Hz
Pulse overlap	30 – 70 %

HPF process was conducted on a 60-tonne hydraulic press machine to form 22MnB5 boron steel blanks of 70 mm width, 140 mm length and 1.8 mm thickness as shown in Figure 3. The HPF process parameters are shown in Table 3. Four thermocouples were attached inside the lower die holder at a 1 mm distance from the die insert surface to measure the temperature distribution within the die subsurface. A data logger was plugged in to record the temperature from the thermocouples during the quenching process. Characterisation of the laser-modified die inserts after performing HPF was carried out for hardness properties. The formed 22MnB5 steel surface was characterised for hardness properties and martensite percentage analysis.

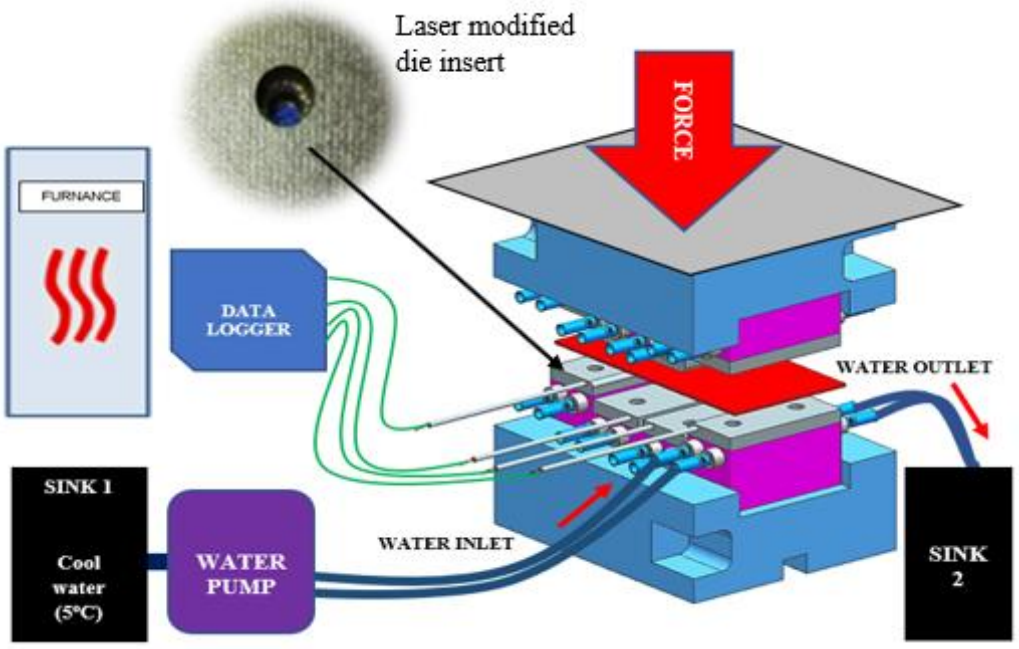

Figure 3: Schematic diagram of the hot press forming process setup.

Table 3: Hot press forming processing parameter.

Hot Press Forming Parameter	
Cooling Temperature	5 °C
Cooling water flow rate	45 L/min
Quenching time	8 s
22MnB5 heating temperature	950 °C
Cooling medium	Water
Distance between upper and lower die	20 mm
Press Machine Pressure	6 MPa

The 22MnB5 sample after the HPF process is shown in Figure 4. After the HPF process, the 22MnB5 blanks sample was characterised for metallographic study, hardness properties and martensite distribution analysis. Hot press formed samples were ground using abrasive paper

with 1200 grit size and were polished using imperial cloth with 1 µm diamond paste before image analysis. Phase transformation was analysed using ImageJ software using the threshold menu.

Figure 4: The 22MnB5 boron steel after the hot press forming processes.

3.0 RESULTS AND DISCUSSION

3.1 Laser Modified Die Inserts Characteristics

The die insert surface after laser modification at various laser parameters is shown in Figure 5. Figures 5(a) to 5(c) show die inserts with laser surface melting at 70, 50 and 30% overlap and their magnified morphology. It took 4.9 to 16.1 minutes to complete the melting process on the die insert at 30 to 70% overlapping respectively.

The micrographs of laser modified cross-section at 6000× magnification are presented in Figure 6. Figure 6(a) shows the formation of three layers after laser processing, namely melted zone (MZ), heat affected zone (HAZ), and substrate. The grain structure of MZ is shown in Figure 6(b). MZ contains a refined, equiaxed grain structure relative to the substrate material where metallurgical changes were due to localised surface heating and rapid solidification of the micron-sized molten pool from the pulsed laser (Bariman et al., 2017), (Pu et al., 2020). Equiaxed grain structure seems to be larger at the centre of the laser melted pool when the cooling process was delayed, which is attributed to the latent heat at a higher cooling rate. Figure 6(c) depicts a coarse grain structure in HAZ, which was attributed to a lower temperature and different temperature heating in the molten pool depth. HAZ is a transition zone where the substrate is partially melted with altered chemical composition due to high temperature processing. While, the temperature between liquidus and solidus causes partial melting in HAZ, resulting in formation of the columnar grain structure or coarser grain (Lv et al., 2024).

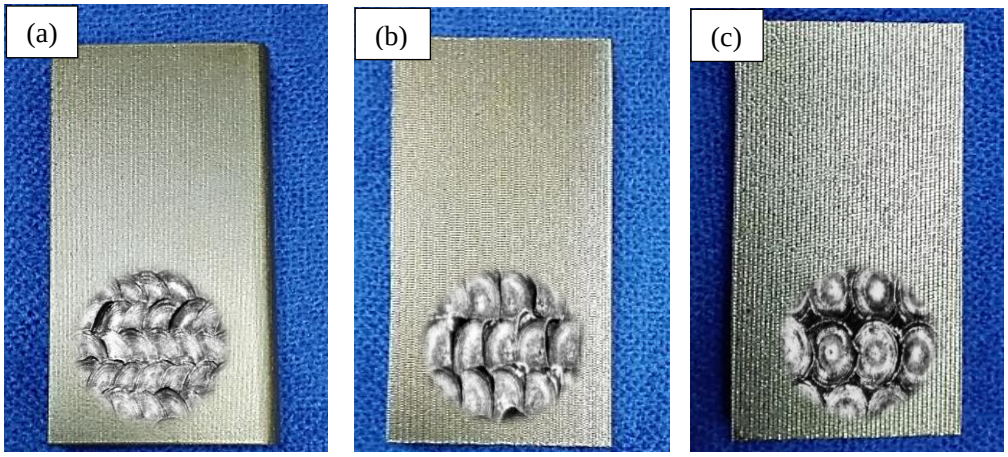

Figure 5: Die insert surface and magnified morphology after laser melting at (a) 70%, (b) 50% and (c) 30% overlap.

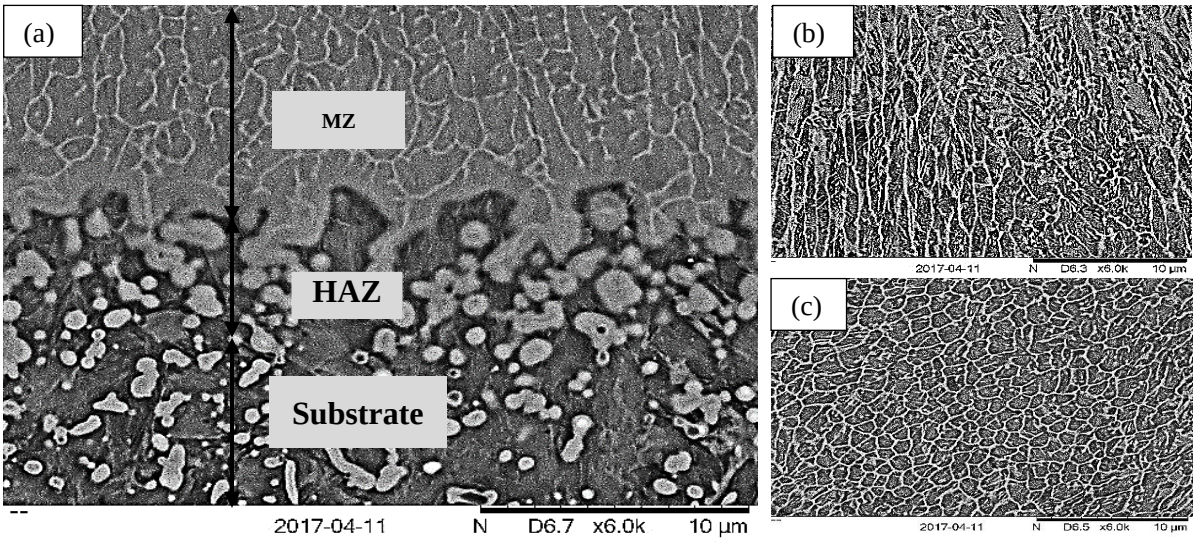

Figure 6: SEM micrographs of (a) laser-modified AISI H13 tool steel cross-section with the presence of melted zone (MZ), heat affected zone (HAZ) and substrate material, (b) columnar grain structure in the HAZ, and (c) fine equiaxed grain structure in the MZ at 6000× magnification.

The grain structure varied according to different melted depths, which was due to the use of different operating temperatures. Figure 7 presents the SEM micrographs of the evolved grain structure of melted die surface in MZ at various overlapping rates. Rapidly melted and solidified H13 die surface yielded smaller grain boundary size in the MZ. The grain boundary structure expanded with the increase of overlapping rates from 30 to 70%, as shown in Figure 7(a) to 7(c). Referring to the figures, grain boundary size decreased as the overlapping rate decreased. The grain at the overlapping rate of 30% in Figure 7(a) was smaller since the lower overlapping rate

produced a faster cooling rate. On the other hand, the grain boundary at the overlapping rate of 70% shown in Figure 7(c) appeared coarser with less boundary, as the slow cooling process in the melted pool increases the grain size. The average grain size in the melted layer was 1.02 μm, while the average grain size in the substrate was 3.02 μm. A high overlapping rate produces slow processing speed, it causes delay solidification on the melted pool and producing a bigger grain size. Figure 7(d) depicts the as-received H13 steel with a ferrite background as well as the presence of carbide phase distribution. The micrograph shows a large grain size with a thin grain boundary in the as-received H13 sample. This study demonstrated that grain refinement in laser-melted layers can be tailored for different grain sizes (Yu et al., 2024).

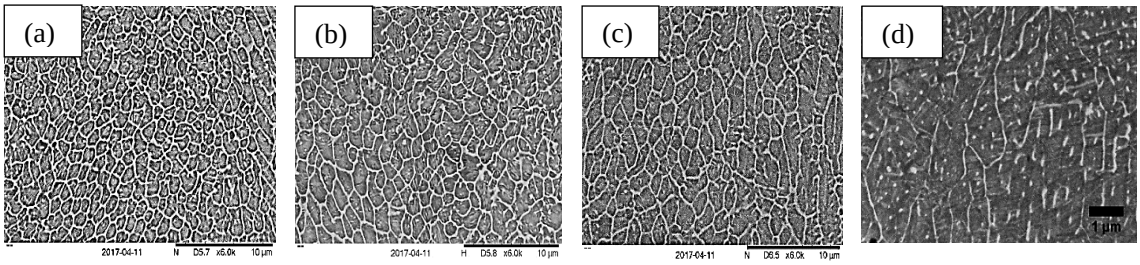

Figure 7: SEM Micrographs of grain structure evolution laser melted zone of AISI H13 samples which were processed at (a) 30%, (b) 50%, (c) 70% overlapping rate at 15000× magnification and (d) as-received H13.

The laser parameters, such as pulse repetition frequency (PRF), peak power, overlapping rate, and average power, demonstrate variations of pulse energy, residence time, and irradiance, which yield different properties of the modified surface. Overall, the depth of the modified layer decreased with increasing PRF due to lower energy penetration. However, changing overlapping rates increased the molten pool depth significantly, as shown in Figure 8. Higher processing speed produced fewer overlapping laser spots, which attributed to the shorter interaction time between the laser beam and sample surface. Thus, the maximum depth of 0.33 mm is obtained at 70% overlap and 50 Hz PRF, which is equivalent to 2 J energy. Laser peak power was found to significantly affect the overlapping laser spots pattern, where high peak power increased the amount of energy absorbed by the surface and consequently produced a deeper molten pool. On the other hand, lower pulsed energy produced lower surface temperature, thus improving surface topography. Meanwhile, a shorter interaction time with high irradiance is required to avoid overheating, burn marks, and spark on the sample surface.

A similar trend obtained at a lower laser energy of 1.43 J resulted from 70 Hz PRF, where the modified layer thickness was doubled when the overlapping rate increased from 30 to 70%; since lower laser penetration reduced the absorption of laser energy into the sample surface. Longer laser-material interaction time was attributed to the reduced processing speed at a higher overlapping rate, consequently producing fully modified sub-surface and deeper molten pools. In some works, the overlapping rate can be achieved by increasing the PRF to a higher range of 2300-3000 Hz; this requires a high laser translation speed range of 2000 mm/min. For this study, slowing the sample speed produces higher overlaps that are applicable for lower-range PRF. The low processing speed allows higher surface temperature that promotes energy penetration and efficient surface melting (Rakesh et al., 2019).

Rapid solidification during laser processing customized the surface morphology, where surface roughness analysis is crucial for considering a better surface finish. The surface roughness at an overlapping rate of 30% was the highest at 3.89 μm, whereas the surface roughness at an overlapping rate of 70% was the lowest at 1.89 μm, which is highly dependent on the speed and peak power. At higher peak power, more laser irradiance is transmitted into the substrate and overheated the surface (Bariman et al., 2017). The overheated surface increased the fluid flow within the molten pool when linearly translated at higher speeds, thus developing rough morphology. Increasing the PRF and residence time reduces the energy and laser-surface interaction, which results in lower surface roughness.

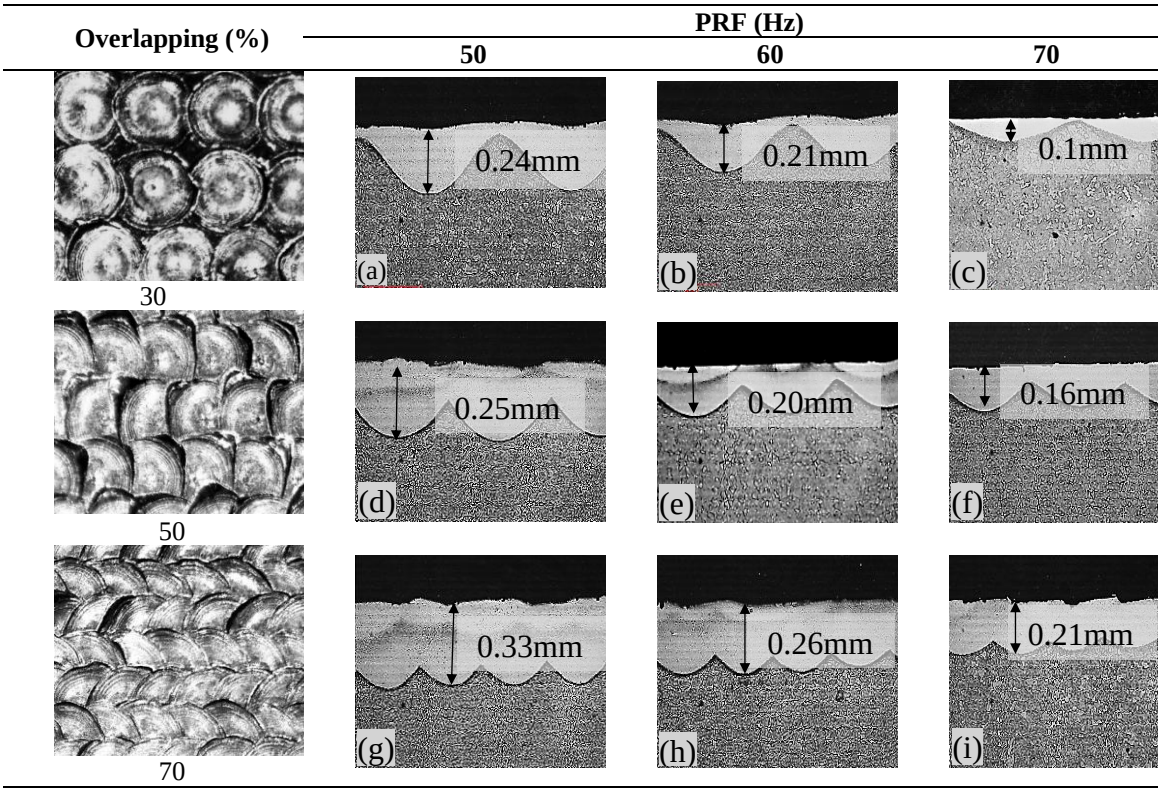

Figure 8: Surface morphology and micrographs of varying molten pool and modified depth at 30%, 50% and 70% overlap with different pulse repetition frequency.

The laser modified sub-surface hardness properties multiplied due to different heating and solidification rates. Heating and solidification rates are significant in laser surface melting to control the size of the microstructurally altered region which complies with the Hall-Petch strengthening. Besides hardness properties, the yield strength of a material increases proportionally with the square root of grain size (Pan et al., 2020). After the laser modification process, a higher number of grains was observed in the affected layer, thus increasing the hardness properties between 684.4 and 793.7 $HV_{0.1}$, as shown in Figure 9. Rapidly melted and solidified H13 surface yield smaller grain size and high-volume fraction of grain boundary in the melted layer, consequently increasing hardness properties. On the other hand, lower hardness

was measured across the HAZ to the substrate due to larger grain size. The highest hardness in sample processed at P_p of 2500 W, PRF of 60 Hz, and 30% overlap, was due to reduced heating time resulting in a higher solidification rate, yielding a smaller grain size in the melted layer. The lowest hardness at the sample processed at 2500 W P_p, 60 Hz PRF, and 70% overlap was due to shorter interaction time between the laser beam and substrate or latent heat that delays the solidification rate. The enhancement of surface hardness is important to improve the wear resistance of the die surface for enhanced lifetime.

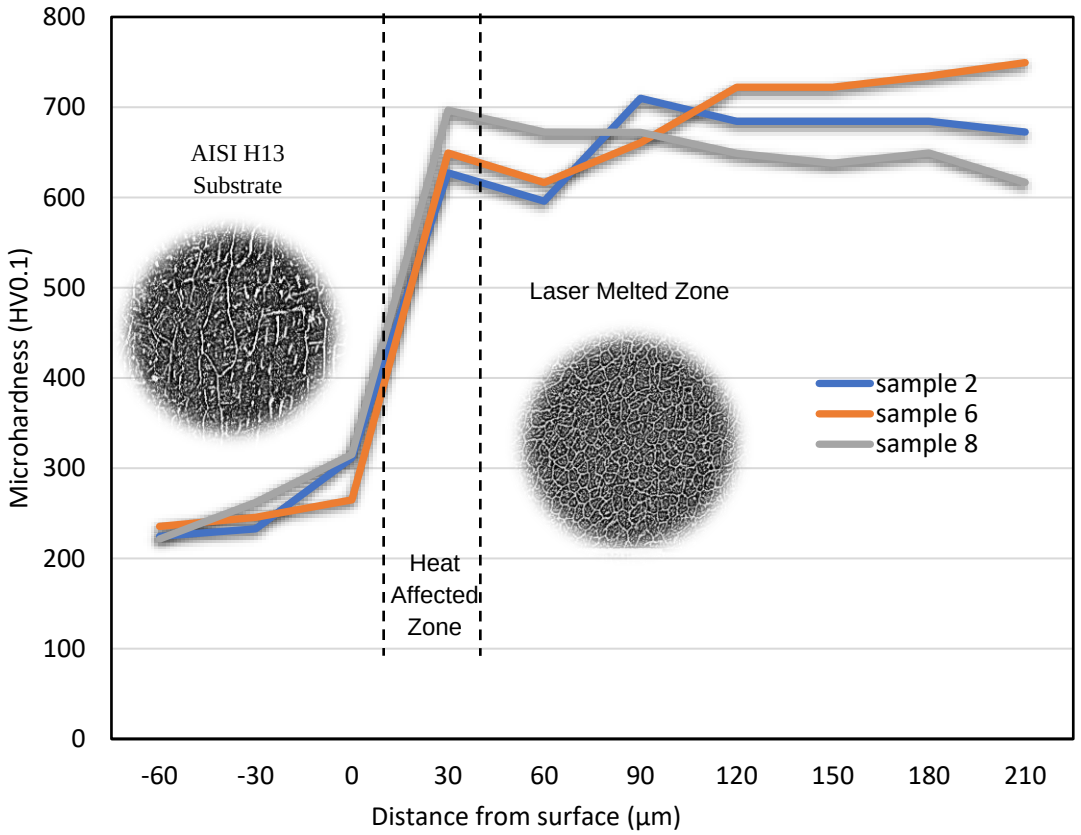

Figure 9: Microhardness properties of laser modified AISI H13 die inserts subsurface at different overlapping rate (sample 2:50%, sample 6:30% and sample 8:70% overlapping rate).

3.2 Characteristics of Hot Press Formed 22MnB5 Steel

The resulted martensitic microstructure of 22MnB5 blank from HPF process is presented by the micrograph in Figure 10(b) and compared with the as-received blank in Figure 10(a). During HPF, the ferrite phase of 22MnB5 blanks transformed into martensite due to quenching effects during forming. Though this finding is predictable in HPF however, the new findings worth emphasised are, martensite structure varies in responding to different laser parameters used to modify the die inserts. From the image threshold analysis, the martensite structure composition in 22MnB5 blanks after forming using as-received die inserts is 58.7%. Whereas, the blanks consist of a higher martensite structure of 80.6% after forming by laser modified inserts with

lower overlapping rates and peak power. The comparison of martensite structure composition analysed from modified inserts at different peak power and overlapping rates can be referred to Figure 11. At 70% overlap, in Figure 11(a) and 11(d), the appearance of the martensite structure is coarser than the martensite structure at 30% overlaps shown in Figure 11(c) and 11(f). A homogenous martensite structure of 78.1% composition was observed in blanks produced from the laser modified die inserts at 30% laser spots overlap and higher peak power of 2500 W.

The tensile strength and hardness properties of 22MnB5 boron steel blanks correspond to the martensitic structure. The martensite structure is the common strengthening component for high strength boron steel. Martensite structure of 80.6% and 74.8% produced high tensile strength up to 1630 MPa and 1520 MPa respectively. Hot press formed 22MnB5 boron steel blanks using as-received H13 die inserts exhibit high strength steel properties with an average hardness of 386.6 $HV_{0.1}$. Whereas the laser modified die inserts multiplied the hardness of 22MnB5 boron steel blanks 508.1 $HV_{0.1}$ which is 2.5 times higher than its as-received condition.

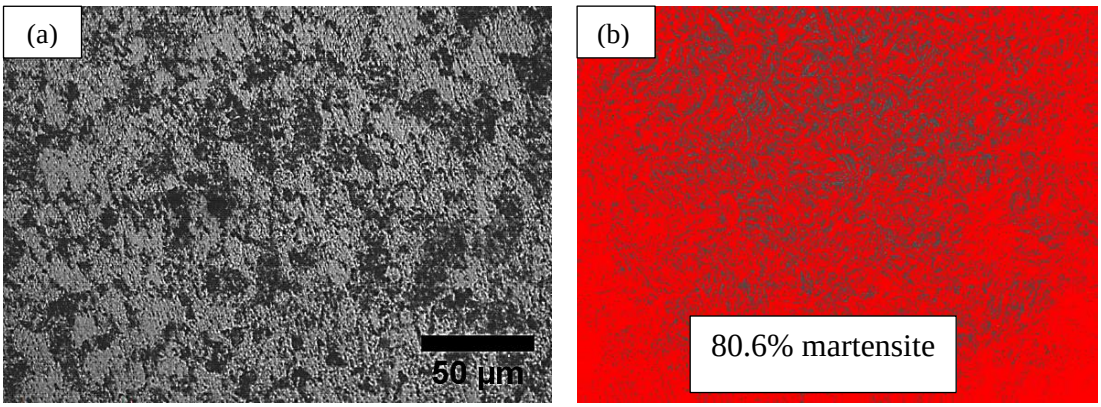

Figure 10: Micrograph of 22MnB5 blank (a) before, and (b) after HPF process.

In most cases, the high thermal conductivity of die materials and die insert surface roughness are among the factors that affect the properties of the blank (Valls et al., 2017). During laser processing, high temperatures during the melting process allowed some elements to diffuse into the melted zone, as shown in Figure 12. The composition recorded by EDXS is summarised from the spectra line, where an increase of several elements was detected in the MZ. The high temperature range diffused the elements and settled near the grain boundary due to rapid solidification (Aqida et al., 2013). The diffusion temperature of carbon elements occurred at a temperature range of 975 to 1075 ℃ (Tibbetts, 1980). Adding to that, high carbon content was detected in the laser-melted layer during the melting process, which enhances hardness properties. In alloys, grain boundaries decrease lattice thermal conductivity by creating microstructural barriers and enhancing phonon scattering (Nagarjuna et al., 2020). However, for refined grain structure, lattice thermal conductivity is affected by element composition. Significant composition changes of manganese (Mn), nickel (Ni), molybdenum (Mo) and chromium (Cr) may have increased the lattice thermal conductivity of laser-modified surface, as these elements diffused to the grain boundaries (Peet et al., 2011).

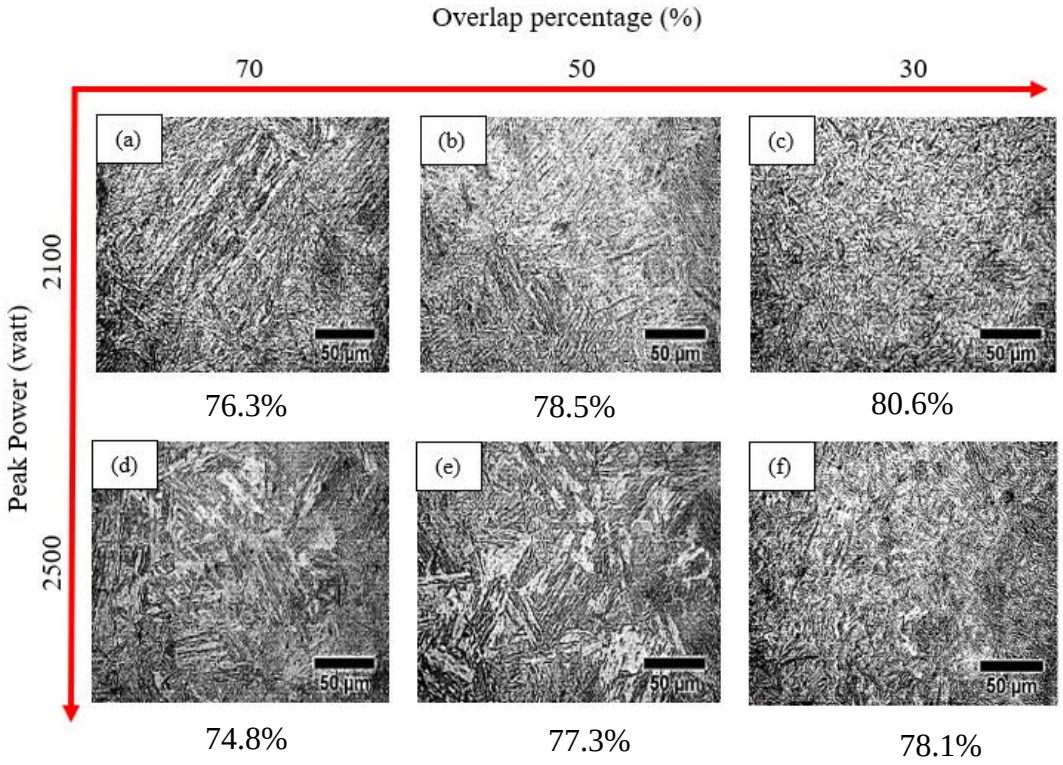

Figure 11: Micrograph of martensite structure composition in 22MnB5 steel blank after hot press forming responding to different laser-modified die insert conditions.

In addition, since the laser-modified inserts surface roughness ranged between 1.89 and 3.89 µm, the die-blank surface contact during HPF process was affected. Less metal-to-metal contact between the die surface and 22MnB5 blank occurred which caused a lubrication effect during quenching (Shihomatsu et al., 2016). The rough surface morphology of the modified die insert surface enhanced the cooling rate. Faster cooling rate in laser-modified die inserts enhanced martensite phase transformation of 22MnB5.

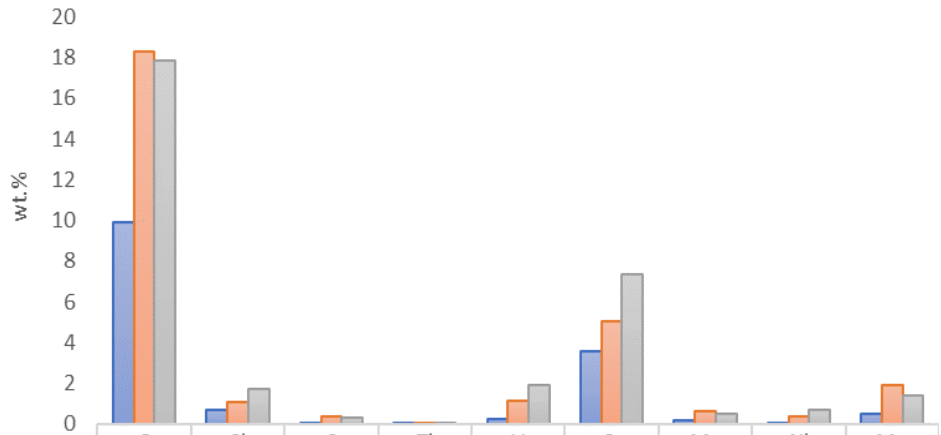

	C	Si	S	Ti	V	Cr	Mn	Ni	Mo
As-received ASSAB 8407	9.907	0.704	0.003	0.006	0.234	3.578	0.143	0.021	0.466
Melted Zone	18.28	1.07	0.379	0.064	1.139	5.058	0.647	0.338	1.895
Heat Affected Zone (HAZ)	17.882	1.717	0.322	0.038	1.892	7.373	0.499	0.655	1.383

Figure 12: Chemical composition summarized of AISI H13 (ASSAB 8407) tool steel in the melted zone and heat affected zone.

The laser modified insert surface comprises a refined grain structure and a high volume fraction of grain boundary. Both grain size and grain boundaries affect thermal conductivity, the smaller grain size has lower thermal conductivity as more grain boundaries obstruct the heat transfer. This is shown by the thermal analysis of die insert during HPF process in Figure 13. The temperature distribution was measured within 1 mm inside the lower die insert surface throughout the hot press forming of 40 pieces of 22MnB5 blanks. The temperature of laser modified die surface stabilized after eight cycles of forming process (that involved a heating and cooling process). The first eight cycles were the transient phase, while the following cycles were at a steady-state phase where the temperature of HPF die inserts is consistent during the forming process. As for the unmodified H13 die insert surface, the temperature distribution was in a steady state after ten cycles. The initial temperature of die inserts was 5 ^{o}C prior to the forming, while the temperature of the austenitized 22MnB5 blank was 950^{o}C.

In particular, Figures 13(a) to 13(d) show the thermal distribution of the unmodified and laser-modified die inserts during HPF process. The average water temperature within 1 mm of the die insert surface at 30%, 50% and 70% overlap was 40.4 ^{o}C, 50.2 ^{o}C and 58.5 ^{o}C, while for the as-received die insert, the average water temperature was at 60.9 ^{o}C. From these results, the unmodified H13 steel inserts absorbed more heat during the quenching process compared to the modified surface inserts. At a lower overlapping rate of 30%, thicker grain boundaries (as shown in Figure 7(a)) become obstacles to the heat transfer which explains the lower temperature of 40.4 ^{o}C in Figure 13(a). Larger grain size in unmodified H13 steel inserts quickly absorbed and released heat, as indicated by respective maximum and minimum temperatures of 60.9 and 20.7 ^{o}C in Figure 13(d).

Although the thermal conductivity of laser-modified surface inserts decreased, the quenching process of blank by die inserts is more efficient due to the rough surface morphology. Higher surface roughness reduced metal-to-metal contact (die surface and 22MnB5) that generated a

lubrication effect for a faster cooling rate. Meanwhile, high hardness modified surface has increased resistance to thermal fatigue. The least heat-affected die insert surface prevents materials from premature degradation and substantial overheating. Increasing the thermal wear resistance of die insert prolonged its lifecycle without compromising the formed blank properties. The temperature history of the unmodified and laser-modified insert surface is shown in Figure 14. The peak temperature was achieved when both upper and lower dies were in close position, with a temperature difference of 33.7%. More rapid heat dissipation occurs in the water flow through the unmodified insert compared to the modified surface inserts.

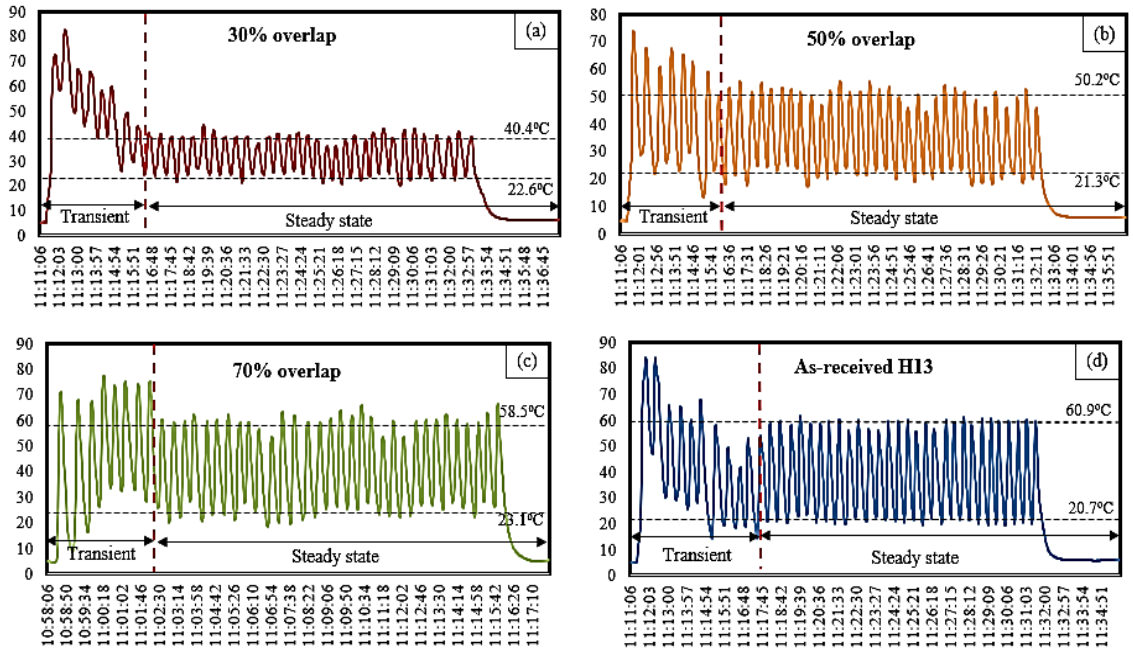

Figure 13: Maximum and minimum thermal distribution in laser modified die insert surface of 30% overlap (a), 50% overlap (b), 70% overlap (c) and; unmodified AISI H13 die insert surface (d) at 40 cycles of HPF.

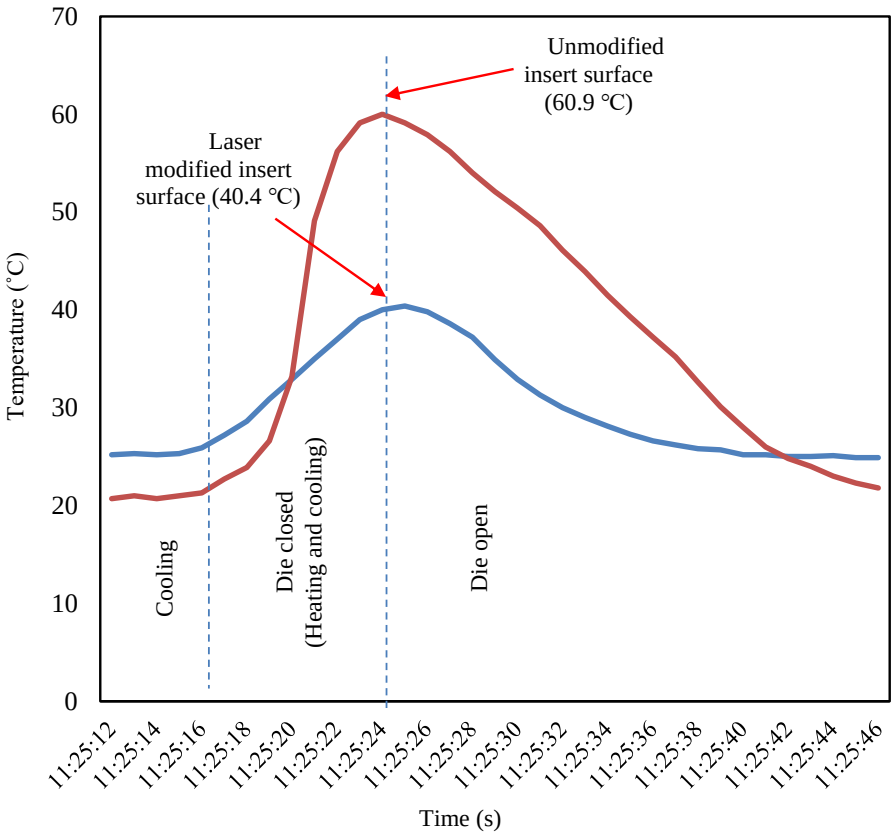

Figure 14: Temperature history of as-received and laser modified die insert surface from HPF process.

3.3 Thermal Stability of Laser-Modified Die Insert After HPF Processes

The laser-modified surface consists of a metastable phase that becomes thermally unstable when exposed to temperatures above 600 ℃. After 40 cycles of hot press forming, the thermal stability of laser-modified insert surface was characterised by its hardness properties. Figure 15 shows the hardness of laser-modified inserts from sample 1 (P_P:2100 W, PRF:50 Hz, overlap:30%) and sample 10 (P_P:2100 W, PRF:70 Hz, overlap:30%) before and after the HPF process. Before the HPF process, samples 1 and 10 exhibited a respective hardness of 778.9 $HV_{0.1}$ and 672.5 $HV_{0.1}$. Both samples experienced a slight increase in hardness to 825.3 $HV_{0.1}$ and 696.7 $HV_{0.1}$ after the HPF process due to the secondary hardening effect during the forming stage (Zhang et al., 2019). Subsequent forming resulted in a temperature-pressure couple effect on the die insert surface from the austenitised blanks. High pressure from the dies during forming, retained the fine grain structure while the cyclic heating enhanced the hardness properties. In the absence of pressure, the grain boundary moved when exposed to high temperature and merged into larger grains with lower hardness.

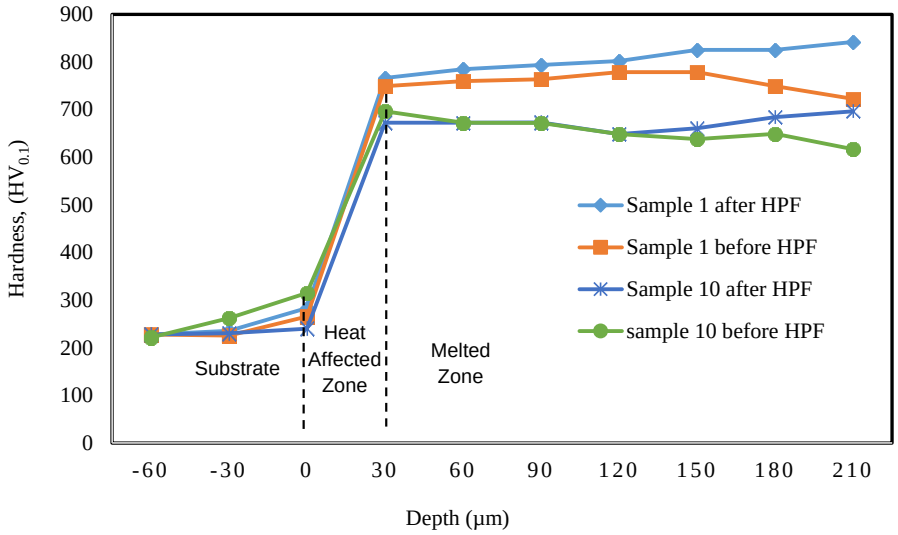

Figure 15: Hardness properties stability of laser-modified die surface before and after HPF of 22MnB5 steel blank as a function of the melted layer depth.

CONCLUSIONS

In this work, the thermal stability of laser-modified surface has been studied for hot press forming die inserts. The following conclusion can be drawn from the findings:

a. Increasing overlapping rate varies the grain structure and grain boundaries volume fraction, thus altering the thermal conductivity of laser modified surface.
b. Rough surface morphology produced by a low overlapping rate significantly increased the martensite structure of 22MnB5 to 80.6%, which displays the hardness properties.
c. The high hardness laser modified surface can be tailored for minimum thermal conductivity and high cooling rate effects for prolonged die inserts lifecycle.
d. The thermal stability of laser-modified die inserts was enhanced by temperature-pressure couple effects by retaining the grain structure when in contact with austenitized blanks at 950 ℃.

ACKNOWLEDGEMENT

The authors would like to acknowledge the financial support from University Malaysia Pahang under Tabung Persidangan Dalam Negara and RDU230398 UMPSA Fundamental Research Grant, Politeknik Sultan Mizan Zainal Abidin for providing advanced machining facility and University Tun Hussein Onn Malaysia for providing the laser facility.

REFERENCES

Aqida, S., Brabazon, D., & Naher, S. (2013). Atomic diffusion in laser surface modified AISI H13 steel. Applied Physics A, 112(1), 139-142.

Aqida, S., Maurel, M., Brabazon, D., Naher, S., & Rosso, M. (2009). Thermal stability of laser treated die material for semi-solid metal forming. International Journal of Material Forming, 2, 761-764.

Bariman, N., Aqida, S. N., & Fauzun, F. (2017). Laser Melting of High Thermal Conductivity Steel (HTCS) Surface. Paper presented at the Materials Science Forum.

Burger, N., Laachachi, A., Ferriol, M., Lutz, M., Toniazzo, V., & Ruch, D. (2016). Review of thermal conductivity in composites: mechanisms, parameters and theory. Progress in Polymer Science, 61, 1-28.

Du, C., Hoefnagels, J., Kölling, S., Geers, M., Sietsma, J., Petrov, R., . . . Amin-Ahmadi, B. (2018). Martensite crystallography and chemistry in dual phase and fully martensitic steels. Materials Characterization, 139, 411-420.

Emamverdian, A. A., Sun, Y., Cao, C., Pruncu, C., & Wang, Y. (2021). Current failure mechanisms and treatment methods of hot forging tools (dies)-a review. Engineering Failure Analysis, 129, 105678.

Fujii, S., Yokoi, T., Fisher, C. A. J., Moriwake, H., & Yoshiya, M. (2020). Quantitative prediction of grain boundary thermal conductivities from local atomic environments. Nature Communications, 11(1), 1854. doi:10.1038/s41467-020-15619-9

Gordillo, N., de Castro, C. G., Tejado, E., Pastor, J., Balabanian, G., Panizo-Laiz, M., . . . del Rio, J. (2017). On the thermal stability of the nanostructured tungsten coatings. Surface and Coatings Technology, 325, 588-593.

Han, Q., & Yi, X. (2022). High pressure-induced elimination of grain size softening in nanocrystalline metals: Grain boundary strengthening overwhelming reduction of intragranular dislocation storage ability. International Journal of Plasticity, 153, 103261.

Liu, X., Laplanche, G., Kostka, A., Fries, S., Pfetzing-Micklich, J., Liu, G., & George, E. (2019). Columnar to equiaxed transition and grain refinement of cast CrCoNi medium-entropy alloy by microalloying with titanium and carbon. Journal of Alloys and Compounds, 775, 1068-1076.

Lv, Y., Cui, B., Sun, Z., & Xiao, X. (2024). Influence of discrete laser surface melting on hot cracking behavior and mechanical properties of Q235 steel. Materials Chemistry and Physics, 325, 129750.

Mori, K., Bariani, P., Behrens, B.-A., Brosius, A., Bruschi, S., Maeno, T., . . . Yanagimoto, J. (2017). Hot stamping of ultra-high strength steel parts. CIRP Annals, 66(2), 755-777.

Nagarjuna, C., Dharmaiah, P., Kim, K. B., & Hong, S.-J. (2020). Grain refinement to improve thermoelectric and mechanical performance in n-type Bi2Te2. 7Se0. 3 alloys. Materials Chemistry and Physics, 256, 123699.

Norhafzan, B., Aqida, S., Chikarakara, E., & Brabazon, D. (2016). Surface modification of AISI H13 tool steel by laser cladding with NiTi powder. Applied Physics A, 122(4), 1-6.

Pan, T., Karnati, S., Zhang, Y., Zhang, X., Hung, C.-H., Li, L., & Liou, F. (2020). Experiment characterization and formulation estimation of tensile properties for selective laser melting manufactured 304L stainless steel. Materials Science and Engineering: A, 798, 140086.

Peet, M., Hasan, H., & Bhadeshia, H. (2011). Prediction of thermal conductivity of steel. International Journal of Heat and Mass Transfer, 54(11-12), 2602-2608.

Pu, Z., Jing, X., Yang, C., Wang, F., & Ehmann, K. F. (2020). Wettability modification of zirconia by laser surface texturing and silanization. International Journal of Applied Ceramic Technology, 17(5), 2182-2192.

Rakesh, K., Bontha, S., Ramesh, M., Das, M., & Balla, V. K. (2019). Laser surface melting of Mg-Zn-Dy alloy for better wettability and corrosion resistance for biodegradable implant applications. Applied Surface Science, 480, 70-82.

Shihomatsu, A., Button, S. T., & Silva, I. B. d. (2016). Tribological behavior of laser textured hot stamping dies. Advances in tribology, 2016.

Sun, Y., Fu, L., Fu, Z., Shan, A., & Lavernia, E. J. (2017). Enhanced thermal stability and ductility in a nanostructured Ni-based alloy. Scripta Materialia, 141, 1-5.

Tibbetts, G. G. (1980). Diffusivity of carbon in iron and steels at high temperatures. Journal of Applied Physics, 51(9), 4813-4816.

Valls, I., Hamasaiid, A., & Padré, A. (2017). High Thermal Conductivity and High Wear Resistance Tool Steels for cost-effective Hot Stamping Tools. Paper presented at the Journal of Physics: Conference Series.

Yu, X., Liu, R., Feng, Q., Liu, L., Zhu, Z., & Wang, B. (2024). Corrosion performance and microstructure of a Q370qENH weathering steel welded joint treated by the laser surface remelting method. Materials Letters, 363, 136319.

Zhang, C., Li, P., Wei, S., You, L., Wang, X., Mao, F., Luo, C. (2019). Effect of tempering temperature on impact wear behavior of 30Cr3Mo2WNi hot-working die steel. Frontiers in Materials, 6, 149.

Zheng, L., Wu, J., Zhang, S., Sun, S., Zhang, Z., Liang, S., Ren, L. (2016). Bionic Coupling of Hardness Gradient to Surface Texture for Improved Anti-wear Properties. Journal of bionic engineering, 13(3), 406-415.